A Model of Inhomogeneous Broadening and Pressure Induced Hole Shifts in the Optical Spectra of Organic Chromophores in Glasses

Indrek Renge*

Institute of Physics, University of Tartu, EE51014 Tartu, Estonia

Received: March 12, 2001; In Final Form: June 6, 2001

Zero phonon holes were burned in the $S_1 \leftarrow S_0$ absorption bands of organic compounds in ethanol glass at 6 K. The application of He gas pressure (P) leads to the shift of holes with a frequency coefficient $d\nu/dP$. The linear dependence of $d\nu/dP$ on hole position (ν) within the inhomogeneous band is of considerable interest, since it can provide the $S_1 \leftarrow S_0$ energies of nonsolvated chromophores and the (local) compressibility of the surrounding matrix. However, the extrapolated frequencies $\nu_{0(P)}$ at which pressure shift should vanish deviate from the actual 0−0 energies of free solutes in a vacuum. The slope (a) of the plot of $d\nu/dP$ vs ν varies between 1.5×10^{-5} and 6.2×10^{-5} bar^{-1} for different dyes, and therefore cannot be directly associated with the isothermal compressibility of the matrix. To account for these facts, a model was developed based on the assumption that the solvent shift is a superposition of repulsive, dispersive, electrostatic, and other possible interactions. Each interaction has a specific intermolecular distance (r) dependence (e.g. r^{-6} for dispersive and r^{-12} for repulsive interactions) and is assigned a Gaussian frequency distribution function. It follows from the model that the observed slope a depends on, in addition to the volume compressibility of the matrix, the widths of the constituent Gaussians and the respective power coefficients of r. Both the measured bandwidth and the slope a are also sensitive to the type of correlation between different solvent shift mechanisms. In rhodamine dyes a dipole moment change between the ground and the excited state is responsible for a strong broadening and a shallow slope a. The conformational flexibility of a dicarbocyanine dye HIDCI has similar consequences. The mechanisms leading to a matrix polarity dependent hypsochromism in open chain cyanine dyes, free base tetrapyrroles, and *s*-tetrazine correspond to a distance dependence of r^{-6} and are deemed to be of multipolar nature. The magnitude of the hypsochromic solvent shift owing to repulsive forces is probably small, although their contribution to the slope a and the inhomogeneous bandwidth may be relatively large.

Introduction

Inhomogeneous broadening of spectroscopic transitions has attracted much interest because of its ubiquitous role in shaping the ensemble spectra.[1−4] In a disordered solid environment the spread of microscopic solvent shifts gives rise to a broad spectral contour with a peak maximum shifted with respect to the vacuum frequency of a nonsolvated species. The narrow band excitation of luminescence[5,6] and hole burning[7] are common stationary methods to reveal the properties of centers selected by their transition energies at low temperatures.

We have recently reported the pressure-induced shifts of spectral holes burned in inhomogeneously broadened absorption bands of many dyes doped in glassy matrices.[8,9] The rather numerous literature data of the past decade have been reviewed and discussed.[9] It was confirmed that optical holes shift proportionally and reversibly with the pressure of gaseous He up to 200 bar. Moreover, the pressure shift coefficients $d\nu/dP$ of purely electronic transitions determined in this way depend linearly on hole frequency ν.[10−14] A frequency at which there is no pressure-induced shift ($\nu_{0(P)}$) can be found either directly or by extrapolation. Earlier the $\nu_{0(P)}$ has been identified with the 0−0 energy of the transition in a vacuum (ν_0). The slope of a linear plot $d\nu/dP$ vs the hole position ν, denoted as a, has been treated in terms of the isothermal (local) compressibility of the matrix (β_T).[12−14]

By contrast, the studies of a single dye, tetra-*tert*-butylporphyrazine, embedded in a number of polymers[8] as well as a large set of π-electronic molecules in a glassy ethanol[9] have shown that the parameters of great interest, ν_0 and β_T, can hardly be derived directly from the experimental plots of $d\nu/dP$ vs ν. The nontrivial behavior of pressure-induced hole shifts means that several mechanisms of solvent shifts, each with different distance dependence, are always operative. A mechanism causing large a values has tentatively been assigned to repulsive interactions that are known to possess extremely steep distance dependence.[8,9] On the other hand, the reaction fields, cavity fields, hydrogen bonding, and conformational flexibility of the dye molecules were identified as inhomogeneous broadening mechanisms causing flat plots of $d\nu/dP$ vs ν with small a. With a few exceptions, broad bands in polar environment have a shallow slope a, whereas the relatively narrow bands of nonpolar systems yield the a values that can be considerably larger than $2\beta_T$. In this paper the inhomogeneous broadening is treated in terms of different microscopic solvent shift mechanisms. The bandwidths and the slopes a are postulated for the repulsive and dispersive interactions, and the contributions of the remaining mechanisms are separated using the statistical properties of Gaussian random variables. It will be demonstrated that the room temperature solvent shift data provide cues to the nature of these extra interactions influencing the bandwidth and pressure shifts of spectral holes.

* Phone: +3727-304800; FAX: +3727-383033; E-mail: renge@fi.tartu.ee

10.1021/jp010928t CCC: $20.00
Published on Web 09/15/2001

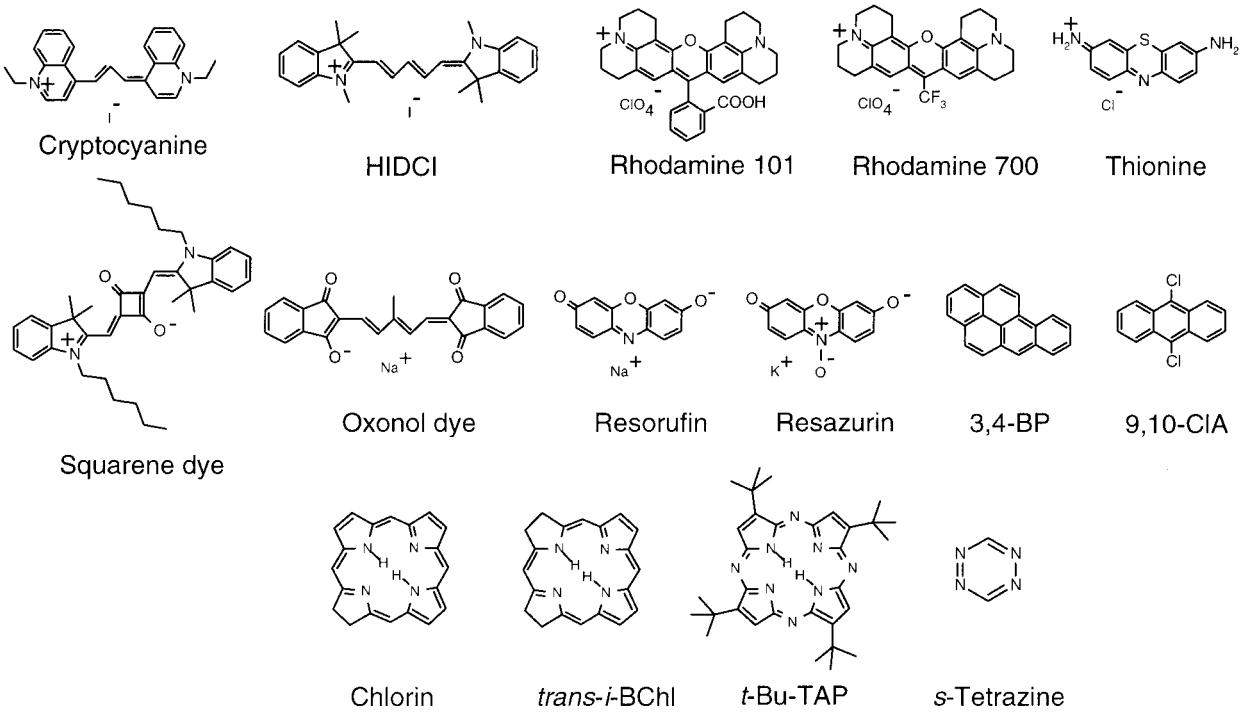

Figure 1. Chemical structures of guest molecules.

Experimental Section

The chemical structures of the chromophores are depicted in Figure 1. The sources of dyes as well as the other details of the measurements have been described recently.[8,9] Most of the data are taken from our previous work.[9] In short, the absorption spectra were recorded on a Perkin-Elmer Lambda 9 spectrophotometer using the 1−10 mm Hellma cells for solutions at room temperature and 0.5−1 mm cells for low-temperature glasses. The hole burning samples were placed in 0.5−1 mm thick open containers made of thin polyethylene film supported by a loop of wire. The pressure cell is made of a stainless steel cylinder of 20 mm in diameter housing a 2-mm thick and 4 mm wide sample room and supplied with two 2-mm thick sapphire windows. The sample frozen at 6 K was slowly pressurized with He gas up to about 200 bar, and the system was let to cool again during 5 min prior to the hole burning. Holes were burned with a Lambda Physik dye laser LPD 3002E pumped with an excimer laser LPX 100. Relatively deep holes broadened (fwhm ~10 GHz) by the high light dose were created at 3 to 5 positions over the band for a pressure run. Holes were explored in a two-channel setup with a Molectron JD2000 Joulemeter ratiometer using averaging over 10 pulses. The influence of pressure change was followed by stepwise releasing of the He gas.

Theoretical Considerations

Following a long standing tradition, the solvent shifts of optical band maxima will be considered as a superposition of partial shifts owing to distinct physical mechanisms.[15−20] For example, the second-order perturbation theory provides four components to the total medium induced shifts due to dipole−dipole, induced dipole−dipole and dispersive interactions.[15,19,20]

1. Single Solvent Shift Mechanism. Let us assume that a given mechanism denoted by I produces a shift $\Delta\nu_I$ when a single chromophore is surrounded with i solvent molecules, each at a distance r_i, contributing a partial shift $\Delta\nu_{Ii}$: $\Delta\nu_I = \sum\Delta\nu_{Ii}$. If the mechanism I has a characteristic intermolecular distance (r^{-n}) dependence one can write

$$\Delta\nu_I = c_I \sum_i r_i^{-n} \tag{1}$$

where c_I is a constant and n is a power coefficient.

The hydrostatic He gas pressure provides a means for fine-tuning the intermolecular spacing in a completely reversible and elastic fashion.[8−14] The pressure (P) shift of the transition frequency is obtained by differentiation of eq 1, bearing in mind that $\Delta\nu_I = \nu_I - \nu_0$ (ν_0 refers to the free chromophore), i.e., $d(\Delta\nu_I) = d\nu_I$:

$$d\nu_I/dP = -nc_I \sum_i [r_i^{-n-1}(dr_i/dP)] \tag{2}$$

Since the linear isothermal compressibility of the system α_T is expressed as $\alpha_T = -(dr_i/dP)_T r_i^{-1}$, one obtains that the pressure shift is proportional to the absolute solvent shift

$$d\nu_I/dP = n\alpha_T \Delta\nu_I \tag{3}$$

In the case of a large ensemble of molecules, the plot of pressure shift coefficients $d\nu_I/dP$ vs the absolute solvent shift $\Delta\nu_I$ or simply the hole position is linear with a slope a_I:

$$a_I = d(d\nu_I/dP)/d\nu_I = n\alpha_T \tag{4}$$

Instead of α_T the isothermal volume (V) compressibility β_T ($\beta_T = -(dV/dP)_T V^{-1}$) of the host matrix is usually applied ($\beta_T = 3\alpha_T$).

Therefore, in an ideal case when a single microscopic solvent shift mechanism is involved, the transition frequency of a nonsolvated dye can be found from the condition $d\nu_I/dP = 0$ (eq 3), and the (local) compressibility can be determined provided the power coefficient n is known (eq 4). According to the London formula, the dispersion attraction energy depends on the intermolecular distance as r^{-6} ($n = 6$) yielding the slope value equal to $2\beta_T$.[8,9,12−14]

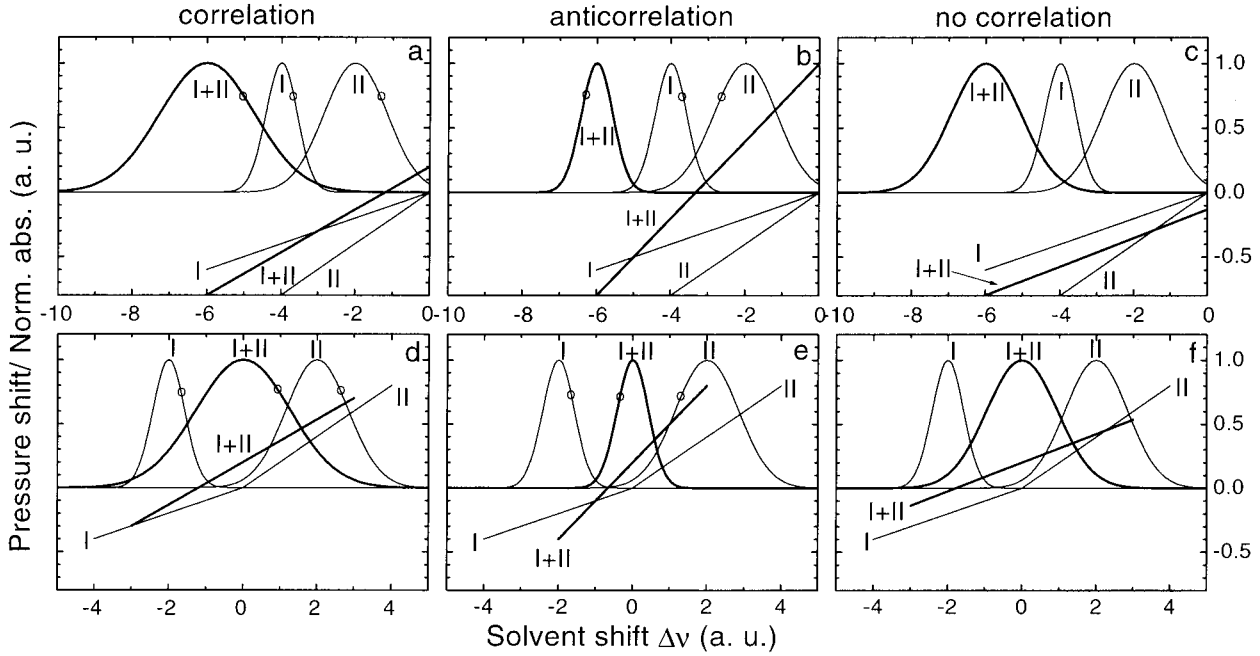

Figure 2. Model of inhomogeneous broadening and pressure shift of an optical transition in a disordered environment. A combination of two solvent shift mechanisms (I and II) is illustrated, each characterized by a solvent shift $\Delta\nu_{maxj}$, a width Γ_j, a pressure shift coefficient a_j, and a type of correlation between them. The upper frames a to c show a case when both mechanisms lead to red (negative) shifts, whereas the lower frames d to f show shifts with different signs. A selected group of centers is marked on the right slope of curve I by "○" and projected to the second spectrum: on the same side to define the correlation and on the opposite one for anticorrelation. The position of marked molecules in anticorrelated superposition (I + II) is on the same side as in the broader spectrum II. The mechanism I has $\Gamma = 1$ and produces a red shift of -4 (a−c) or -2 (d−f) units, whereas the mechanism II has broader spectrum with $\Gamma = 2$ that is displaced to the red by -2 (a−c) or to the blue by 2 units (d−f). The shift $\Delta\nu$ is obtained as a sum of partial shifts (eq 7). The resulting width is a sum in the case of correlation (a,d) (eq 8), a difference in the case of anticorrelation (b,e) (eq 9), and a convolution in the absence of correlation (c,f) (eq 10). The pressure shifts are proportional to $\Delta\nu$ and have slopes a 0.1 and 0.2 for the I and the II mechanisms (thin lines), respectively. The combined slope (thick lines) depends on the type of correlation and the bandwidths, but not on shifts (eqs 11−13). The pressure shift for a composite band at $\Delta\nu = 0$ is generally not equal to zero.

2. Several Solvent Shift Mechanisms. Experimentally, a linear relationship between the pressure shift coefficient $d\nu/dP$ and the burning frequency ν holds indeed (eq 3), and the wavenumber at which the P shift vanishes ($\nu_{0(P)}$) can be found either directly or by extrapolation:[8−14]

$$d\nu/dP = a(\nu - \nu_{0(P)}) \tag{5}$$

As a rule, poor correspondence between the 0−0 origin of the free chromophore ν_0 and the extrapolated no-pressure shift frequency $\nu_{0(P)}$ was observed.[8,9] Further, the slope a does not remain constant for various guest molecules doped in poly(methyl methacrylate) (PMMA)[8] or ethanol glass.[9] Such deviations are by no means surprising, since at least two intermolecular interaction mechanisms, a repulsive and an attractive one, must operate simultaneously, each with different distance dependence between the solute and solvent molecules. The interaction radii or the power coefficients n for the repulsive and dispersive forces as well as electrostatic interactions can be very different.

The absorption band, or more precisely, the inhomogeneous distribution function (IDF), of transition energies can be treated as a superposition of Gaussian curves, each corresponding to a solvent shift mechanism with a characteristic distance dependence. Our aim is to express the observables: the bandwidth and the maximum position, the pressure shift at the band maximum and the slope coefficient a in terms of the widths and displacements of constituent Gaussians and the respective power coefficients n.

For simplicity, let us assume that two different interaction types (numbered by j; j = I, II, ...) can be represented by Gaussian distributions with a relative probability density y_j, a full width at half-maximum Γ_j and a peak displacement $\Delta\nu_{maxj}$ with respect to the transition frequency in a vacuum ν_0 (Figure 2):

$$y_I = \exp -[1.665(\nu - \Delta\nu_{maxI})/\Gamma_I]^2 \tag{6a}$$

The curves are scaled by a factor of $2(\ln 2)^{1/2} = 1.665$ to have

$$y_{II} = \exp -[1.665(\nu - \Delta\nu_{maxII})/\Gamma_{II}]^2 \tag{6b}$$

$(\nu - \Delta\nu_{maxj})$ equal to $1/2\Gamma_j$ at $y_j = 0.5$.

The Gaussians (eq 6a and 6b) ought to be treated as statistical random variables to obtain the resultant spectrum.[21] The positions of band maxima simply add up:

$$\Delta\nu_{max} = \Delta\nu_{maxI} + \Delta\nu_{maxII} \tag{7}$$

When dealing with bandwidths, the correlation between the solvent shifts must be considered. In Figure 2 three cases are illustrated: perfect correlation, perfect anticorrelation (which is also a correlation!), and the statistically independent Gaussian variables. Ideal correlation means the equality of heights ($y_I = y_{II}$) at the same side of the curves eqs 6a and eq 6b. In this case the bandwidths add up (Figure 2a and d):

$$\Gamma = \Gamma_I + \Gamma_{II} \tag{8}$$

The anticorrelation, defined as $y_I = y_{II}$ at the opposite sides of the curves eqs 6a and 6b, leads to the narrowing of the resulting spectrum (Figure 2b and e):

$$\Gamma = \Gamma_{II} - \Gamma_I, \text{ (if } \Gamma_{II} > \Gamma_I) \tag{9}$$

The anticorrelation and the accompanying narrowing may seem unrealistic. However, it is conceivable that a large dispersive red shift of the centers in a closely packed surrounding ($\Delta\nu_{disp} \ll 0$) corresponds to large frequency upshift ($\Delta\nu_{rep} \gg 0$) via the repulsive mechanism (Figure 2e).

Finally, in the absence of correlation, the resulting spectrum is a convolution of Gaussians (eqs 6a and 6b; Figure 2c and f):

$$\Gamma = (\Gamma_I^2 + \Gamma_{II}^2)^{1/2} \tag{10}$$

For a single mechanism, the linear dependence of pressure shift coefficients $d\nu_j/dP$ on hole burning frequency extrapolates to zero at vacuum frequency ν_0 and has a slope a_j (eq 3, Figure 2, thin lines). The slope coefficient a of a composite band depends on widths and slopes of every interaction type as follows:

$$a = (a_I\Gamma_I + a_{II}\Gamma_{II})/(\Gamma_I + \Gamma_{II}) \text{ for correlation} \tag{11}$$

$$a = (a_{II}\Gamma_{II} - a_I\Gamma_I)/(\Gamma_{II} - \Gamma_I), \text{ if } \Gamma_{II} > \Gamma_I, \text{ for anticorrelation} \tag{12}$$

$$a = 1/2(a_I\Gamma_I + a_{II}\Gamma_{II})/(\Gamma_I^2 + \Gamma_{II}^2)^{1/2} \text{ for the lack of correlation} \tag{13}$$

Irrespective to the type of correlation, the pressure shift coefficient measured for a hole burned at the absorption maximum $d\nu_{max}/dP$ can be calculated on the basis of the partial solvent shifts $\Delta\nu_{maxj}$ and slopes a_j:

$$d\nu_{max}/dP = d\nu_{maxI}/dP + d\nu_{maxII}/dP = a_I\Delta\nu_{maxI} + a_{II}\Delta\nu_{maxII} \tag{14}$$

As far as we adhere to the separability of intermolecular interactions, our ultimate goal would be the splitting of the measured spectra into (Gaussian) constituents of specified widths and displacements. If only two interactions are involved, with the respective slopes a_j and the type of correlation known, the calculation of four unknown parameters (Γ_I, Γ_{II}, $\Delta\nu_{maxI}$, $\Delta\nu_{maxII}$) would be possible from the measured bandwidth Γ and shift $\Delta\nu_{max}$ together with the slope a and $d\nu_{max}/dP$ values by using eqs 7 to 14. However, in a polar ethanol host matrix the number of interactions is definitely larger than two. In the following, the forces other than dispersive attraction and exchange repulsion will be discussed in more detail using the low and high (ambient) temperature absorption spectra and the pressure shifts of spectral holes.

Results

1. Solvent Shifts at Room Temperature. In contrast to solids, the properties of liquids can be modified over a broad range simply by choosing solvents with different dielectric permittivities (ϵ) and refractive indices (n). The influence of these variables on optical transitions is conventionally treated in terms of dielectric continuum models.[15,19,20] The effects of temperature and repulsive interactions are assumed to be either negligible or to remain constant in different solvents. Here we utilize the room temperature solvent shifts in order to separate the dispersive and the polarity dependent shifts and to estimate the vacuum frequencies ν_0 that are inaccessible from supersonic jet data.

The spectral shifts in nonpolar solvents, particularly *n*-alkanes are described very well with Bakhshiev equation that uses the average static polarizability difference ($\alpha_e - \alpha_g$) between the ground and the excited state[15,22,23]

$$\nu = \nu_0 + p\phi(n^2)$$

$$p = -3II'(\alpha_e - \alpha_g)/[2(I + I')r^3] \tag{15}$$

where $\phi(n^2)$ is the Lorentz−Lorenz function ($\phi(n^2) = (n^2 - 1)/(n^2 + 2)$), I and I' are the ionization energies of the solute and solvent molecules and r is the Onsager cavity radius.

The plots of band maxima in *n*-alkanes vs the Lorentz−Lorenz function $\phi(n^2)$ are perfectly linear with correlation coefficients larger than 0.99 (Figure 3a) (see Table 2 in ref 9).[22,23] The solvent shift in liquid or solid alkanes will be considered as purely dispersive, since the electronic polarization of the matrix with solute dipole moments is small for chromophores under discussion.[15,22] The slopes p, referred to as Bakhshiev numbers are collected in Table 1. The 0−0 origins of nonsolvated guest molecules ν_0 are estimated from the intercepts of eq 15 (Table 2).[23] The dispersive shifts and the vacuum frequencies of ionic compounds that are insoluble in hydrocarbons were investigated in highly polar aprotic solvents with gradually changing refractive index (Figure 3b).[9,23] In this case the correlation coefficient is lower and the vacuum frequency should be corrected for the dielectric shift.

Although the Bakhshiev numbers that measure the solvent polarizability effect are rather uniform in polymethine dyes (Table 1), the influence of polarity and protic character of the solvent on band maxima depend strongly on the chemical nature of the compound. The red shift for rhodamines in polar media may be caused by a reaction field if the dipoles in the ground and the excited state are parallel and the latter is much larger: $\mu_e > \mu_g$.[15] For rhodamine 6G, the difference between μ_g and μ_e as large as 4.6 D has been reported.[28] The open-chain structures, both cationic (HIDCI, see Figure 3b and cryptocyanine) and anionic (oxonol) display hypsochromism in polar solvents. The partial charges on alternating polymethine atoms may produce some ordering of the solvent dipoles that makes up a reaction field of higher multipolar character.[23,29] Since in the excited state the charges are shifted to the neighboring atoms, extra energy is needed to carry out work against the existing reaction field.

The influence of hydrogen bonds can be demonstrated by comparing the protic and aprotic environments with similar n and ϵ, such as methanol and acetonitrile or ethanol and acetone. In the dicarbocyanine dye HIDCI the H-bonding effect is nearly negligible (Figure 3b). A most pronounced displacement of band maxima by 300−500 cm^{-1} to the higher energies is observed for H-bonded cyclic polymethine anions such as resorufin and resazurin in alcohols.[9]

Polycyclic aromatic hydrocarbons exhibit presumably the simplest solvatochromic behavior with prevailing dispersive red shift. The Bakshiev number lies in the range of −1000 to 2000 and −4000 to 5000 cm^{-1} for ^1L_b (α) and ^1L_a (p) types of transitions in alternant hydrocarbons, respectively.[22,30]

Most of the free-base tetrapyrroles possess large zero phonon transition probability (the Debye−Waller factor) and an intrinsic phototransformation mechanism, and therefore are ideally suited for hole burning studies. However, the dispersive shifts of the S_1 (Q_y) band in free-base tetrapyrroles are small, and nontrivial mechanisms are responsible for the band shift and broadening.[9,31] The blue shift in polar solvents is probably connected with the mutual approach of central protons if the electrostatic repulsion is screened by the medium.[31] We illustrate an irregular case, a reduced porphine, trans-*iso*-bacteriochlorin (trans-*i*-BChl) that is characterized by a rather large dispersive effect with $p = -2176$ cm^{-1} (Figure 3a). By contrast to the other free-base

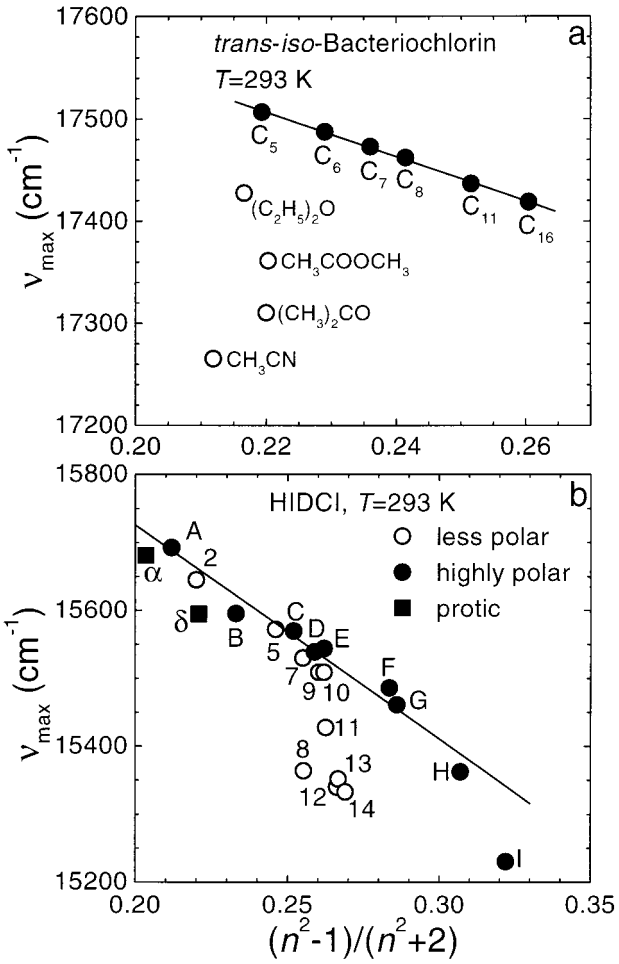

Figure 3. Dependence of $S_1 \leftarrow S_0$ absorption band maxima of *trans-iso*-bacteriochlorin (a) and HIDCI (b) on Lorentz−Lorenz function of solvents at room temperature (eq 15). Normal alkanes are marked as C_n, where n is the number of carbon atoms. Solvents in panel (b) are denoted as in Table 1 in ref 9. Less polar solvents: 2, acetone; 5, tetrahydrofuran; 7, bromoethane; 8, dichloromethane; 9, 1-bromopropane; 10, cyclopentanone; 11, epichlorhydrin; 12, 1,2-dichloroethane; 13, chloroform; 14, $CCl_3COOC_2H_5$. Highly polar solvents: A, acetonitrile; B, nitromethane; C, propylene carbonate; D, dimethylformamide; E, γ-butyrolactone; F, dimethyl sulfoxide; G, sulfolane; H, furfural; I, nitrobenzene. Protic solvents: α, CH_3OH; δ, C_2H_5OH. The lines are linear regressions for *n*-alkanes (a) and solvents A−H (b), the slopes and intercepts are given in Tables 1 and 2.

tetrapyrroles, there is a bathochromic shift of the S_1 band as large as -250 cm^{-1} between *n*-pentane and acetonitrile (Figure 3a). This anomaly is perhaps associated either with central H atoms or bond dipoles, since the overall dipole moment change of trans-*i*-BChl ($\Delta\mu = 1.64$ D)[32] is likely to be responsible only for a minor reaction field shift. Finally, a hypsochromism of electrostatic origin for a $n-\pi^*$ transition of *s*-tetrazine in polar solvents should be mentioned.[9]

2. Absorption Maxima in Ethanol Glass at 6 K. It is difficult to reveal the polarity effects of solid EtOH by direct comparison with a hydrocarbon glass such as 3-methylpentane for two reasons: first, the insolubility of ionic dyes in an apolar medium and second, the lack of knowledge of precise refractive indices (or densities) for vitreous solvents. Instead, the shifts of band maxima in EtOH glass are compared with shifts in a nonpolar matrix of similar index of refraction $\Delta\nu_{disp}$ calculated as $p\phi(n^2)$ (eq 15, Figure 4a, Table 2). The Lorentz−Lorenz function of EtOH glass was assumed to be 0.28, by 25% larger than that of the room-temperature liquid.

For polyarenes and several tetrapyrroles and polymethines the observed and calculated band shifts virtually coincide (Figure 4a). The deviations owing to the polarity of ethanol are apparent as a blue shift is in cryptocyanine (255 cm^{-1}), HIDCI (318 cm^{-1}), oxonol dye (354 cm^{-1}), *t*-Bu-TAP (180 cm^{-1}), and *s*-tetrazine (204 and 458 cm^{-1} for two solvate complexes) (Table 2). The observed solvent shift is also much less than 0.28*p* in resorufin (by 372 cm^{-1}) and resazurin (by 777 cm^{-1}) due to the hydrogen bonding. On the other hand, a bathochromic shift occurs in rhodamine 700 (-260 cm^{-1}) because of its polarity and in thionine (-405 cm^{-1}) as a result of hydrogen bonding.

As expected, there is an approximate correspondence between the residual nondispersive shift calculated as a difference between $\Delta\nu_{max}$ and 0.28*p* in solid EtOH (Table 2) and the polarity-dependent solvent shifts in liquid solvents at 293 K (previous section, for details see ref 9).

3. Inhomogeneous Broadening in Ethanol Glass. The shapes of inhomogeneous site distribution functions (IDF) can be determined by selective spectroscopy methods.[18,33−36] The half-widths at half-maximum on the long wavelength slope (hwhm) will be discussed here for simplicity. For most of the compounds, the 0−0 bands are well separated from the vibronic satellite bands, the Debye−Waller factors are relatively large, from 0.3 to 0.8 (that corresponds to the Huang−Rhys factors from 1.2 to 0.2), and the phonon frequencies are small, so that Γ (= 2hwhm) coincides with the width of IDF within 20%.

In polycyclic arenes, a roughly linear dependence between the bandwidth Γ and the absolute solvent shift of the peak maximum $\Delta\nu_{max}$ holds in EtOH:[9,37]

$$\Gamma = (108 \pm 8) - (0.087 \pm 0.007)\Delta\nu_{max};\ N = 3,\ r = 0.9967 \quad (16)$$

Therefore, the bandwidth is ∼0.1 of the dispersive shift plus a residual value of ∼100 cm^{-1}.

The other compounds have spectra broader than alternant polyarenes (Table 1). A question arises whether this additional broadening is correlated with the peak shift as in the case of dispersive interaction. Obviously, every microscopic mechanism capable of displacing the center of gravity of the ensemble spectrum produces inhomogeneous broadening in a disordered environment. The opposite is definitely not true. For example, the linear Stark effect on a polar transition occurring in a randomly oriented cavity field would produce a spread of transition energies but no average shift. Another mechanism of inhomogeneous broadening that may be accompanied with negligible shift arises as a result of conformational flexibility of chromophores.

The excessive broadening in dipolar rhodamines 700 and 101, and probably in trans-*iso*-bacteriochlorin and resazurin is caused by a linear Stark shift in static solvent cavity fields of different magnitude and direction.[9] The broadening in the oxonol and HIDCI as compared to cryptocyanine and the squarene dye stems from the conformational flexibility of the pentamethine chain in the former structures. The procedure of separating the contributions of different broadening mechanisms will be outlined in the Discussion section.

4. Dependence of Pressure Shift Coefficient on Hole Frequency. The pressure shift coefficient dν/dP of a spectral hole depends strongly on the burning position within the inhomogeneous spectral contour (the so-called color effect, refs 8−14) (Figures 5 and 6). The slopes a of the linear plots of dν/dP vs the hole burning frequency (ν) are collected in Table 2. Inspection of Table 2 reveals that the slope varies between 1.5×10^{-5} and 6.2×10^{-5} bar^{-1} in a single matrix, solid EtOH,

TABLE 1: Contributions to the Inhomogeneous Bandwidth of Guest Molecules in Ethanol Glass at 6 K

guest	$-p$ (cm^{-1})[a]	Γ (cm^{-1})[b]	Γ_{disp} (cm^{-1})[c]	Γ_{rep} (cm^{-1})[d]	Γ_{III} (cm^{-1})[e]
		Polymethine Compounds			
cryptocyanine I^-	3024 ± 286[f]	222	85	(100)	123
HIDC I^-	3156 ± 241[f]	382	88	(100)	333
rhodamine 101 ClO_4^-	3027 ± 245[f]	460	85	(100)	421
rhodamine 700 ClO_4^-	2577 ± 120[f]	466	72	(100)	433
thionine Cl^-	3680 ± 681[f]	282	103	(100)	196
squarene dye	2617 ± 84	204	73	(100)	108
oxonol dye Na^+	3634 ± 274[f]	308	102	(100)	233
resorufin Na^+	2435 ± 481[f]	212	68	(100)	129
resazurin K^+	1594 ± 831[f]	340	45	(100)	308
		Polycyclic Aromatic Hydrocarbons			
3,4-benzopyrene	1567 ± 60	146	44	66	96
3,4-benzopyrene[g]		110	44	66	0
9,10-dichloroanthracene	4175[h]	218	117	57	131
9,10-dichloroanthracene[g]		174	117	57	0
		Tetrapyrrolic Compounds			
chlorin	659 ± 20	136	19	(100)	66
trans-iso-bacteriochlorin	2176 ± 46	412	61	(100)	379
tetra-*tert*-butylporphyrazine	988 ± 39	188	28	108	130
tetra-*tert*-butylporphyrazine[g]		136	28	108	0
		Azaarene with $n-\pi^*$ Transition			
tetrazine[i]	1062 ± 23	216	30	(100)	172
		201		(100)	153

[a] Bakshiev number from ref 9. [b] Double value of the half-width at half-maximum (2 hwhm) measured at the long wavelength slope of the band. [c] Dispersive contribution to the broadening, equal to 10% of the dispersive shift $\Gamma_{disp} = -0.028p$. [d] Repulsive contribution to the broadening. [e] Contributions to the broadening of electrostatic and other mechanisms calculated as from eq 18. [f] Measured in very polar aprotic solvents. [g] In 3-methylpentane glass. [h] For anthracene. [i] Parameters for the two Gaussian components of the absorption band.

TABLE 2: Experimental and Calculated Solvent and Pressure Shifts of Guest Molecules in Ethanol Glass at 6 K

guest	ν_0 (cm^{-1})[a]	$\Delta\nu_{max}$ (cm^{-1})[b]	$\Delta\nu_{disp}$ (cm^{-1})[c]	$\Delta\nu_{max} - \Delta\nu_{disp}$ (cm^{-1})[d]	$d\nu_{max}/dP$ (GHz/bar)[e]	$(d\nu_{max}/dP)_{disp}$ (GHz/bar)[f]	a ($10^{-5}bar^{-1}$)[g]	a_{III} ($10^{-5}bar^{-1}$)[h]
				Polymethine Compounds				
cryptocyanine I^-	14630 ± 100	−592	−847	255	−0.088	−0.762	3.38	3.2
HIDC I^-	16060 ± 100	−566	−884	318	−0.091	−0.796	2.14	1.5
rhodamine 101 ClO_4^-	17995 ± 66	−760	−848	88	−0.564	−0.763	1.69	1.1
rhodamine 700 ClO_4^-	16230 ± 100	−982	−722	−260	−0.565	−0.65	1.46	0.8
thionine Cl^-	17780 ± 200	−1435	−1030	−405	−0.55	−0.927	2.07	(−0.3)
squarene dye	16353 ± 20	−739	−733	−6	−0.268	−0.66	3.67	4.3
oxonol dye Na^+	15340 ± 100	−664	−1018	354	−0.124	−0.916	3.21	3.3
resorufin Na^+	17590 ± 200	−310	−682	372	−0.196	−0.614	4.25	6.2
resazurin K^+	16192 ± 218	331	−446	777	0.275	−0.401	2.39	2.5
				Polycyclic Aromatic Hydrocarbons				
3,4-benzopyrene	25265[i]	−441	−439	−2	−0.256	−0.395	6.19	
9,10-dichloroanthracene	25950[i]	−1209	−1169	−40	−0.875	−1.052	4.75	
				Tetrapyrrolic Compounds				
chlorin	15912[i]	−101	−185	84	−0.076	−0.167	3.34	3.0
trans-iso-bacteriochlorin	17985 ± 11	−725	−609	−116	−0.43	−0.548	3.45	5.0
tetra-*tert*-butylporphyrazine	16326 ± 9	−97	−277	180	−0.202	−0.249	3.08	2.6
				Azaarene with $n-\pi^*$ Transition				
tetrazine[j]	18128[i]	161	−297	458	−0.054	−0.276	2.92	2.8
		−93		204	−0.117		3.00	2.8

[a] Transition frequency of the nonsolvated dye from eq 15 (ref 9). [b] Absolute solvent shift of the absorption band maximum $\nu_{max} - \nu_0$. [c] Dispersive contribution to the solvent shift calculated as $0.28p$. [d] Solvent shifts other than dispersive. [e] Pressure shift coefficient at the band maximum (ref 9). [f] Dispersive component of the pressure shift coefficient calculated as $2\beta_T\Delta\nu_{disp}$. [g] Slope of the plot of $d\nu/dP$ vs hole position (ref 9). [h] Slope of the plot of $d\nu/dP$ vs solvent shift caused by mechanisms other than dispersion and repulsion interactions (eq 20). [i] In supersonic jets (refs 24−27). [j] Parameters for the two Gaussian components of the absorption band (Figure 5).

and cannot therefore be directly related to a matrix parameter, such as compressibility. In general, broadband spectra seem to have shallow slopes and vice versa.[9,37]

The slopes are particularly shallow in HIDCI (2.14×10^{-5} bar^{-1}) and rhodamines 101 (1.69×10^{-5} bar^{-1}) and 700 (1.46×10^{-5} bar^{-1}). As mentioned above, the larger bandwidth of HIDCI (382 cm^{-1}) with respect to cryptocyanine (222 cm^{-1}) arises perhaps from geometric distortions of the π-electronic system in the former. If the conformers with different transition energies have similar dispersive shifts, a low value of a would result. In rhodamines the spectra are broadened due to linear Stark effect in the cavity field. Under external pressure, the cavity field changes in proportion with linear compressibility α_T equal to $1/3\beta_T$ and the respective slope factor will be shallow.[8,9]

The sensitivity of pressure shifts with respect to the hole frequency is the highest in polycyclic arenes displaying the slope factors as large as $(5-6) \times 10^{-5}$ bar^{-1}. Also, resorufin (4.25),

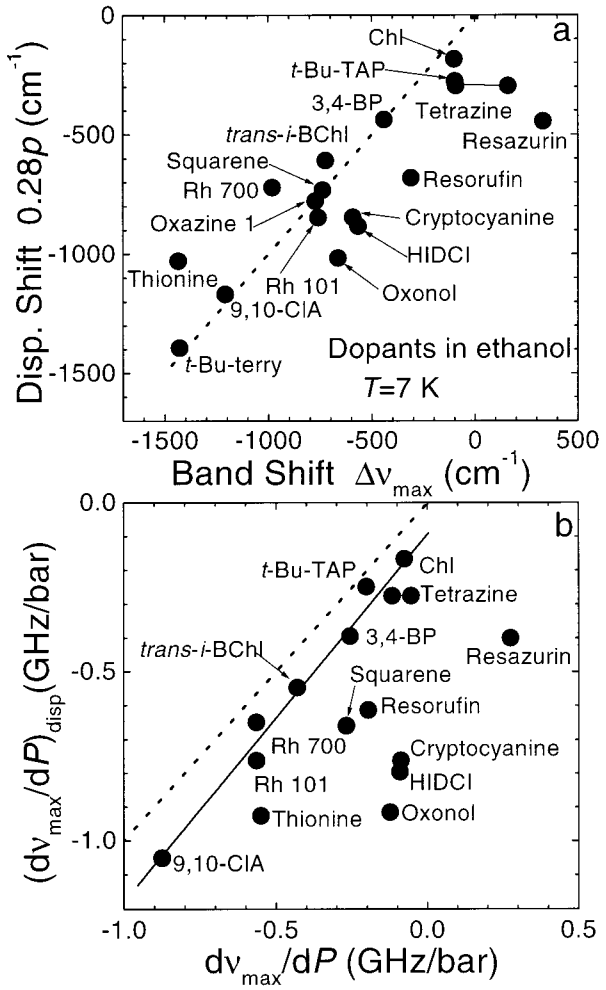

Figure 4. Experimental parameters of the spectra in ethanol glass at 6 K compared with the respective values for pure dispersive shifts. (a) Vacuum-to-matrix shifts of band maxima vs the shifts calculated from the Bakhshiev number p and the matrix polarizability ($\phi(n^2) = 0.28$) as $p(\phi(n^2))$. (b) Pressure shift coefficients of spectral holes burned at the absorption band maxima plotted vs the dispersive contribution (Table 2). The linear regression line (eq 23) is shown. Also, lines with unit slope are drawn for comparison (dashed). Deviations from the dashed lines reveal the influence of additional solvent shift mechanisms.

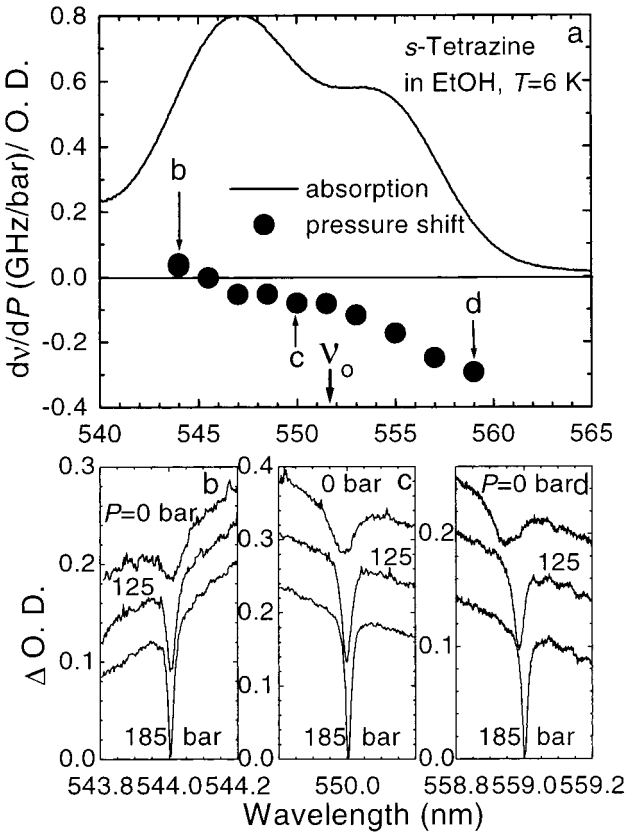

Figure 5. Absorption spectrum and the pressure shift coefficients of spectral holes for *s*-tetrazine doped in EtOH glass measured in a 0.5 mm layer at 6 K (a). The two bands belong to distinct solvational complexes that have been deconvoluted into Gaussians (Tables 1 and 2). The predominant hydrogen bonded species is blue shifted with respect to the 0−0 origin of free *s*-tetrazine at 551.6 nm (ref 27) (indicated by arrow). The holes were burned at the He gas pressure of 185 bar with a light dose of 1.6 J/cm^2 (0.2 mJ/cm^2 per pulse, 100 Hz frequency during 80 s). The broadening and shift of holes after the release of pressure is illustrated in panels (b) to (d). Note that the pressure shift changes sign at 545.5 nm.

the squarene dye (3.67), trans-*i*-BChl (3.45), cryptocyanine (3.38), and chlorin (3.34) possess slopes somewhat larger than the probable $2\beta_T$ of EtOH glass (3.0) (all in 10^{-5} bar^{-1} units). As in the case of PMMA host matrix, the involvement of repulsive potentials will be surmised in order to account for the steep slopes.[8]

Discussion

1. Inhomogeneous Bandwidths. The glasses have a density of about 90% of the crystal phase and contain ∼10% of free volume.[38] The average number of solvent molecules in van der Waals contact with a dye molecule is in the order of ten. A vacancy in the first coordination sphere would correspond to a transition energy change of one-tenth of the total solvent shift $\sim 0.1\Delta\nu_{max}$. Therefore, as a result of polarizability fluctuations in a glass, a broadening equal to 10% of the dispersive shift is expected (eq 15, Table 1):

$$\Gamma_{disp} = -0.028p \qquad (17)$$

The width of polyarene spectra in aliphatic hydrocarbon host glasses exceeding this value (eq 17) may be tentatively attributed to repulsive interactions. Thus, in a completely nonpolar glass, 3-methylpentane (3-MePe), the difference between the measured bandwidth Γ and Γ_{disp} equals to 66 cm^{-1} for 3,4-BP, 57 cm^{-1} for 9,10-ClA, and 108 cm^{-1} for *t*-Bu-TAP (Table 1). Strictly speaking, these values may not correspond to the exact magnitude of Γ_{rep} (eqs 8−10), since, first, we do not know the type of correlation between the interactions, and second, the presence of "third" interactions (e.g., bond dipoles) cannot be rigorously ruled out even in glassy saturated hydrocarbons.

In EtOH the inhomogeneous bands are broader than in 3-MePe: by 36 cm^{-1} for 3,4-BP, 44 cm^{-1} for 9,10-ClA, and 52 cm^{-1} for *t*-Bu-TAP. This additional broadening in EtOH is due to polarity. Since the density dependent mechanisms are hardly correlated with local electric fields, eq 10 should be applied to find out the amount of extra broadening in EtOH (Table 1):

$$\Gamma_{III} = [\Gamma^2 - (\Gamma_{disp} + \Gamma_{rep})^2]^{1/2} \qquad (18)$$

Instead of the sum $\Gamma_{disp} + \Gamma_{rep}$, it is better to use the experimental values of Γ for 3-MePe, if available. For the remaining guest molecules that were poorly soluble in 3-MePe, the Γ_{rep} was taken equal to 100 cm^{-1} and the Γ_{III} was estimated from eq 18. The contribution of electrostatic mechanisms calculated from eq 18 are larger than those obtained by simple

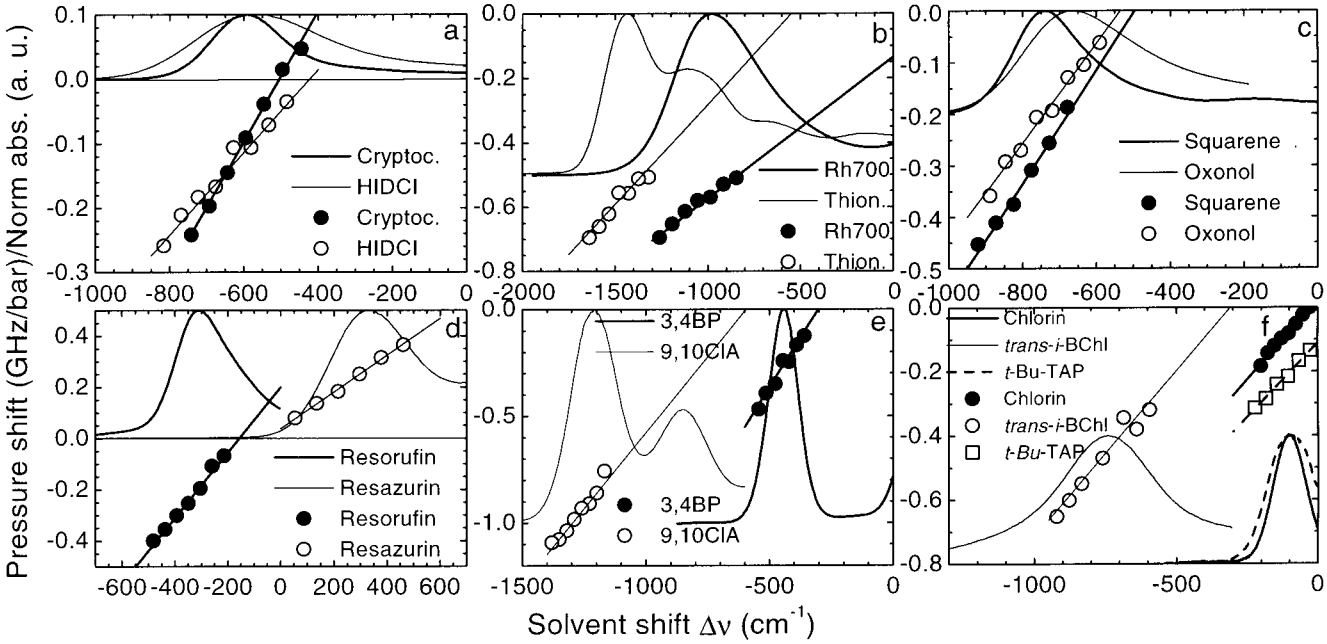

Figure 6. Absorption spectra and pressure shift coefficients of spectral holes for polymethine dyes (a−d), polycyclic hydrocarbons (e), and tetrapyrrolic pigments (f) in ethanol glass at 6 K plotted in a wavenumber scale relative to the 0−0 origins of nonsolvated chromophors.

subtraction: 96 cm^{-1} in 3,4-BP, 131 cm^{-1} in 9,10-ClA, and 130 cm^{-1} in *t*-Bu-TAP (Table 1). Particularly large Γ_{III} values were obtained for Rh 700 (433 cm^{-1}), Rh 101 (421 cm^{-1}), trans-*i*-BChl (379 cm^{-1}), HIDCI (333 cm^{-1}), resazurin (308 cm^{-1}), the oxonol dye (233 cm^{-1}), and thionine (196 cm^{-1}). The Γ_{III} incorporates in addition to the electrostatic contributions (in Rh 700, Rh 101 and trans-*i*-BChl, and probably in resazurin and thionine) the influence conformational (in HIDCI and oxonol dye) and hydrogen bonding effects (probably in thionine and resazurin).

2. Dependence of Pressure Shift Coefficient on Hole Frequency. Each solvent shift mechanism has a characteristic intermolecular interaction radius. The Lennard-Jones function gives the distance dependencies r^{-6} and r^{-12} for attractive and repulsive potentials, respectively. The corresponding slopes of the plots of $d\nu/dP$ vs ν (a) are therefore equal either to two or four times of isothermal volume compressibility β_T of the host matrix (eq 4). According to eqs 11−13, the observed a is a function of widths rather than shifts of the inhomogeneous spectral components. Thus, the slope for a nonpolar system in the case of correlation between the mechanisms can be expressed as

$$a_{disp,rep} = (a_{disp}\Gamma_{disp} + a_{rep}\Gamma_{rep})/(\Gamma_{disp} + \Gamma_{rep}) \qquad (19)$$

From eq 19 it becomes clear that the slope values between a_{disp} ($2\beta_T$) and a_{rep} ($4\beta_T$) could be observed. Moreover, in the case of perfect anticorrelation between the two mechanisms, the resulting slope can be larger than the largest component (eq 12, Figure 2e).

The compressibilities of solvent glasses are not known at low temperatures. Since the pressure induced hole shifts in *t*-Bu-TAP have yielded correct compressibilities for amorphous polymers, the same dye was used to estimate β_T of EtOH, yielding the value of 1.5×10^{-5} bar^{-1}.[8,9] Therefore, the probable values of a_{disp} and a_{rep} are 3×10^{-5} and 6×10^{-5} bar^{-1}, respectively. However, the measured slope in 3,4-BP (6.19×10^{-5}) is even steeper than a_{rep}, despite the fact that the additional electrostatic broadening (Γ_{III}) in ethanol should diminish the resultant slope. We regard this fact as an indication of the expected (partial) anticorrelation between the density-dependent mechanisms, dispersion, and repulsion.

The extra broadening caused by Stark and other interactions Γ_{III} can be very large, exceeding the sum of Γ_{disp} and Γ_{rep} by a factor of 2 (in HIDCI, Rh 101, Rh 700, resazurin, and trans-*i*-BChl). It is of great interest to learn more about the nature of these interactions by determining their distance dependence. As these forces are perhaps weakly correlated with density-dependent attraction and repulsion, the slope a_{III} may be calculated from eq 13:

$$a_{III} = [2a\Gamma - a_{disp,rep}(\Gamma_{disp} + \Gamma_{rep})]/\Gamma_{III} \qquad (20)$$

Because of the expected mutual relationship between the repulsive and dispersive interactions, it seems acceptable to assign $a_{disp,rep}$ a universal value of $\sim 6 \times 10^{-5}$ bar^{-1} that is characteristic for polyarenes in ethanol glass. Then the a_{III} can be estimated from eq 20 using the bandwidths and the observed a from Tables 1 and 2. The power coefficient of the "third" interactions in ethanol glass may be deduced from eq 4 on the basis of a_{III} and compressibility ($\beta_T = 1.5 \times 10^{-5}$ bar^{-1}):

$$n_{III} = a_{III}/0.5 \times 10^{-5} \qquad (21)$$

The lowest slopes a_{III} of $(0.8-1.1) \times 10^{-5}$ bar^{-1} (Table 2) belong to cyclic polymethine cations Rh 101 and Rh 700 that possess appreciable dipole moments both in the ground and the excited state. The distance dependence of $\sim r^{-2}$ (eq 21) points to a long range interaction. As already mentioned, the extensive broadening in rhodamines is likely due to linear Stark shifts in stochastic fields of fluctuating size and direction. It is evident that cavity and reaction fields occur in superposition and both cause broadening, whereas only the latter can lead to a net band shift (−260 cm^{-1} in Rh 700, see Table 2). Under the external pressure the increase of the local field strength is proportional to the linear compressibility ($= 1/3\beta_T$) of the system, giving a distance dependence of r^{-1} that is even less than that predicted from eq 21.

The S_1 transition of cryptocyanine, oxonol dye, the free-base tetrapyrroles chlorin, and *t*-Bu-TAP, as well as a n-π^* chro-

mophore, *s*-tetrazine, undergo pronounced hypsochromic shifts in polar solvents accompanied by an extra broadening in polar EtOH. The calculated a_{III} of about 3×10^{-5} is very similar to that of the London forces, with the power coefficient of the intermolecular separation n_{III} equal to 6. Thus, relatively short-range interactions are responsible for band broadening and solvatochromism in these pigments.

As compared to cryptocyanine ($\Gamma = 222$ cm^{-1}), the dicarbocyanine HIDCI has a much broader spectrum with Γ equal to 382 cm^{-1}. This extra broadening Γ_{III} equal to 333 cm^{-1} (vs 123 cm^{-1} in cryptocyanine) is accompanied with a much smaller a_{III} 1.5×10^{-5} bar^{-1} than in cryptocyanine (3.2×10^{-5} bar^{-1}). Obviously, an additional broadening mechanism comes into play in HIDCI. Distortion of a flexible long-chain chromophore can result in a multitude of conformations with different 0−0 frequencies in a vacuum. The slope *a* will be rendered shallow if the conformers have similar pressure (and solvent) shifts. In this case the inhomogeneous broadening arises as a result of different vacuum frequencies of the conformers.

3. The Magnitudes of Pressure Shift Coefficients at Peak Maxima. The pressure shift coefficients $d\nu_{max}/dP$ of the holes burned at the absorption maxima can be calculated on the basis of partial solvent shifts and slopes:

$$d\nu_{max}/dP = a_{disp}\Delta\nu_{disp} + a_{rep}\Delta\nu_{rep} + a_{III}\Delta\nu_{III} \qquad (22)$$

In Table 2 and Figure 4b $d\nu_{max}/dP$ is compared with the dispersive contribution calculated as $a_{disp}\Delta\nu_{disp}$ ($a_{disp} = 3 \times 10^{-5}$ bar^{-1}; $\Delta\nu_{disp} = 0.28p$). For rhodamines, polyarenes, and tetrapyrroles, a linear relationship between the measured and calculated values is obtained:

$$(d\nu_{max}/dP)_{disp} = -(0.09 \pm 0.03) + (1.09 \pm 0.07) \times (d\nu_{max}/dP),\ N = 8,\ r = 0.988 \qquad (23)$$

The experimental shifts are all slightly less negative than the purely dispersive shifts. Among the chromophores with much less negative pressure shifts are the above-mentioned groups with blue-shifted spectra: the open-chain polymethines, the hydrogen bonded resorufin and resazurin, and the blue form of *s*-tetrazine. The positive (blue) shift mechanisms of multipolar origin have a high value of a_{III} of about 3×10^{-5}(see previous section) and can therefore compensate effectively the negative value of $(d\nu_{max}/dP)_{disp}$.

In a totally nonpolar matrix $\Delta\nu_{III} = 0$ and eqs 7 and 22 may be used for the estimation of repulsive solvent shift $\Delta\nu_{rep}$. At the same time, $\Delta\nu_{disp}$ can be obtained without relying on the liquid-phase Bakshiev number *p*:

$$d\nu_{max}/dP = a_{disp}\Delta\nu_{disp} + a_{rep}\Delta\nu_{rep} \qquad (24)$$

$$\Delta\nu_{max} = \Delta\nu_{disp} + \Delta\nu_{rep} \qquad (25)$$

Unfortunately, it is difficult to examine nonpolar systems, since the hydrocarbon glasses doped with polyarenes are not subject to permanent hole burning. If the polarity-induced shifts in EtOH are ignored (they cannot be specified since the exact refractive indices for solvent glasses are not available), eqs 24 and 25 yield $\Delta\nu_{disp}$ amounting to −598 cm^{-1} for 3,4-BP and −1446 cm^{-1} for 9,10-ClA, which compare well with $0.28p$ (−441 and −1209 cm^{-1}). The calculated $\Delta\nu_{rep}$ is equal to 157 and 237 cm^{-1} for 3,4-BP and 9,10-ClA, respectively. Thus, the repulsive forces seem to cause a small hypsochromism in polycyclic hydrocarbons. The attractive interaction of dispersive origin and the repulsive one have different signs and behave as (partially) anticorrelated mechanisms as illustrated in Figure 2e. The impurity molecules that are tightly surrounded by solvent molecules undergo simultaneously both a large negative dispersive shift and a large positive repulsive shift (and vice versa).

Conclusions

Optical spectra of organic chromophores are severely broadened in frozen solvent glasses and polymer matrices. The energy-selected groups of molecules can be sampled by burning zero-phonon holes in the inhomogeneous site distribution function. Upon application of external pressure, the holes are subject to a shift and a broadening. The very fact of hole broadening means that at least two solvent shift mechanisms are always involved, each with a different dependence on intermolecular distances.[3] The experimental band shape is usually close to a Gaussian that can be split into constituents with characteristic inhomogeneous widths and absolute shifts. Each one would correspond to a distinct mechanism with an intermolecular distance dependence r^{-n}.

A model is proposed in order to assess the shifts and widths due to individual mechanisms by using the pressure shift coefficients measured over the whole band. The main result is that the slope of the pressure shift coefficient vs the burning wavenumber depends on the widths of constituent bands. The slope *a* is independent of the macroscopic solvent shifts produced by each mechanism. By contrast, the magnitude of the pressure shift coefficient at the absorption peak position is a function of individual solvent shifts caused by each mechanism. Both *a* and $d\nu_{max}/dP$ are the functions of individual a_j that in their turn are expressed in terms of power coefficients *n* and the compressibility β_T of the matrix. The model explains why, in general, the extrapolated frequency at which the pressure shift vanishes does not coincide with the vacuum frequency ν_0, although for a single mechanism this would be the case.

Pressure shifts of spectral holes burned in the 0−0 band of polymethine dyes, polycyclic hydrocarbons, tetrapyrrolic pigments, and a $n-\pi^*$ transition of *s*-tetrazine were examined in a polar host, glassy ethanol at 6 K. The aim was to characterize the microscopic solvent shift mechanisms other than dispersive attraction and repulsive forces. The estimated shifts and widths of dispersive origin rely on the room-temperature solvatochromism, and these are approximated to the values of $0.28p$ and $-0.028p$, respectively. The dispersive and repulsive interactions have been assigned the distance dependencies of r^{-6} and r^{-12}, respectively. Further, a probable value of 100 cm^{-1} is used as the repulsive bandwidth for most of the chromophores. As for the repulsive shift, it seems to be small (∼150 cm^{-1}) and hypsochromic.

The characteristics of mechanisms other than repulsive and the London forces in a polar glass may be summarized as follows. The open chain polymethines (cryptocyanine cation, oxonol anion) carry charges of very different magnitudes on neighboring carbon atoms that flip upon excitation. The hypsochromism and broadening in these dyes seem to be due to a multipolar potential with r^{-6}. In another open-chain polymethine, HIDCI, this interaction is also operative as demonstrated by a blue shift in polar solvents. In addition, a huge extra broadening caused by conformational flexibility of HIDCI leads to a small experimental slope factor *a*. The solvent polarity dependent interaction in *n*-tetrazine and the interaction with protons in the center of free-base tetrapyrroles are characterized also by a power coefficient −6. Transitions whose energies are affected by cavity or reaction fields give rise to small slopes, corresponding to $n = 2$. It is worth mentioning that the internal

electric field strength must be proportional to linear compressibility or, in other words to r^{-1} ($n = 1$).

We believe that the concept of separability of intermolecular interactions is applicable for disentangling the fairly complex spectroscopic behavior of disordered solids and liquids. Reliable knowledge of the bulk properties of molecular glasses such as densities, indices of refraction, compressibilities, thermal expansion coefficients, heat capacities, etc. would greatly facilitate the interpretation of optical spectra.

Acknowledgment. I thank Professor Urs P. Wild for kind hospitality during my stay in Physical Chemistry Laboratory, Swiss Federal Institute of Technology (ETHZ), Zürich, Switzerland, where this study was started. This work was supported in part by the Estonian Science Foundation grant No 4511.

References and Notes

(1) Stoneham, A. M. *Rev. Mod. Phys.* **1969**, *41*, 82.
(2) Lee, H. W. H.; Walsh, C. A.; Fayer, M. D. *J. Chem. Phys*. **1985**, *82*, 3948.
(3) Laird, B. B.; Skinner, J. L. *J. Chem. Phys*. **1989**, *90*, 3274.
(4) Sevian, H. M.; Skinner, J. L. *Theor. Chim. Acta* **1992**, *82*, 29.
(5) Personov, R. I. In *Spectroscopy and Excitation Dynamics of Condensed Molecular Systems*; Agranovich, V. M., Hochstrasser, R. M., Eds.; North-Holland: Amsterdam, 1983, Chapter 10.
(6) *Shpol'skii Spectroscopy and Other Site Selection Methods: Application in Environmental Analysis, Bioanalytical Chemistry and Chemical Physics*; *Chemical Analysis, A Series of Monographs on Analytical Chemistry and Its Applications*; Ariese, F., Gooijer, C. Hofstraat, J. W., Eds.; John Wiley: New York, 2000; Vol. 156, 552 pp.
(7) *Persistent Spectral Hole-Burning: Science and Applications*; Moerner, W. E., Ed.; Springer: Berlin, 1988.
(8) Renge, I. *J. Phys. Chem. A* **2000**, *104*, 3869.
(9) Renge, I. *J. Phys. Chem. A* **2000**, *104*, 7452.
(10) Richter, W.; Reul, S.; Haarer, D. *Cryogenics* **1991**, *31*, 223.
(11) Reul, S.; Richter, W.; Haarer, D. *Chem. Phys. Lett.* **1991**, *180*, 1.
(12) Gradl, G.; Zollfrank, J.; Breinl, W.; Friedrich, J. *J. Chem. Phys*. **1991**, *94*, 7619.
(13) Zollfrank, J.; Friedrich, J. *J. Phys. Chem*. **1992**, *96*, 7889.
(14) Pschierer, H.; Friedrich, J.; Falk, H.; Schmitzberger, W. *J. Phys. Chem*. **1993**, *97*, 6902.
(15) Bakshiev, N. G.; Girin, O. P.; Piterskaya, I. V. *Opt. Spektrosk*. **1968**, *24*, 901 (*Opt. Spectrosc*. **1968**, *24*, 483).
(16) Koppel, I. A.; Palm, V. A. In *Advances in Linear Free Energy Relationships*; Chapman, N. B., Shorter, J., Eds.; Plenum Press: London, 1972; pp 203−280.
(17) Renge, I.; Mölder, U.; Koppel, I. *Spectrochim. Acta A* **1985**, *41*, 967.
(18) Renge, I.; Wild, U. P. *J. Lumin*. **1996**, *66 & 67*, 305.
(19) Basu, S. *Adv. Quantum Chem*. **1964**, *1*, 145.
(20) Amos, A. T.; Burrows, B. L. *Adv. Quantum Chem*. **1973**, *7*, 289.
(21) Goodman, J. W. *Statistical Optics*; John Wiley: New York, 1985, 550 pp.
(22) Renge, I. *Chem. Phys*. **1992**, *167*, 173.
(23) Renge, I. *J. Photochem. Photobiol. A* **1992**, *69*, 135.
(24) Greenblatt, G. D.; Nissani, E.; Zaroura, E.; Haas, Y. *J. Phys. Chem*. **1987**, *91*, 570.
(25) Hirayama, S.; Iuchi, Y.; Tanaka, F.; Shobatake, K. *Chem. Phys*. **1990**, *144*, 401.
(26) Even, U.; Jortner, J. *J. Chem. Phys*. **1982**, *77*, 4391.
(27) Smalley, R. E.; Wharton, L.; Levi, D. H.; Chandler, D. W. *J. Chem. Phys*. **1978**, *68*, 2487.
(28) Dubinin, N. V.; Blinov, L. M.; Yablonskii, S. V. *Opt. Spektrosk*. **1978**, *44*, 807 (*Opt. Spectrosc*. **1978**, *44*, 473).
(29) Ghoneim, N.; Suppan, P. *Spectrochim. Acta A* **1995**, *51*, 1043.
(30) Renge, I.; Wild, U. P. In ref 6, pp 19−71.
(31) Renge, I. *J. Phys. Chem*. **1993**, *97*, 6582.
(32) Johnson, L. W.; Murphy, M. D.; Pope, C.; Foresti, M.; Lombardi, J. R. *J. Chem. Phys*. **1987**, *86*, 4335.
(33) Ahn, J. S.; Kanematsu, Y.; Kushida, T. *Phys. Rev. B* **1993**, *48*, 9058.
(34) Tamm, T. B.; Kikas, Ya. V.;. Sirk, A. É. *Zh. Prikl. Spektr*. **1976**, *24*, 315 (*J. Appl. Spectrosc*. **1976**, *24*, 218).
(35) Kikas, J. V.; Treshchalov, A. B. *Chem. Phys. Lett*. **1983**, *98*, 295.
(36) Jaaniso, R.; Kikas, J. *Chem. Phys. Lett*. **1986**, *123*, 169.
(37) Renge, I.; Wild, U. P. *J. Lumin*. **2000**, *86*, 241.
(38) Elliott, S. R. *Physics of Amorphous Materials*; Longman Scientific: Harlow, 1990.